Robust Load Frequency Control with Dynamic Demand Response for Deregulated Power Systems Considering Communication Delays

Qi Zhu[1], L. Jiang[1], Wei Yao[2], Chuan-ke Zhang[3], Cheng Luo[4]

[1]Department of Electrical Engineering and Electronics, University of Liverpool, Liverpool, L69 3GJ, UK.
[2]State Key Laboratory of Advanced Electromagnetic Engineering and Technology, Huazhong University of Science and Technology, Wuhan, 430074, China.
[3]School of Automation, China University of Geosciences, Wuhan 430074, China.
[4]Midwest Independent Transmission System Operator Inc. (MISO), Carmel, Indiana, IN 46032, USA.

Abstract: Communication networks are used in load frequency control (LFC) for transmitting remote measurements and control commands, and in demand side response (DSR) for aggregating small-scale controllable loads. This paper investigates modeling and controller design for LFC together DSR in a deregulated environment, considering multiple time delays introduced by the usage of communication channels. Time delay model of the deregulated multi-area LFC with dynamic demand control (DDC) is obtained at first, in which a typical thermostatically controlled appliance, air conditioner, is used for DDC. A robust proportional integral derivative (PID) load frequency controller is designed, through the H_∞ performance analysis and the particle swarm optimization (PSO) searching algorithm, to deal with the load disturbances and multiple delays in the LFC loop and the DDC loop. Case studies based on a three-area deregulated LFC system demonstrate the effectiveness of the proposed load frequency controller and the performance improvement from the DDC. Simulation results show that the DDC can increase the delay margin of the LFC scheme. Moreover, several delay stable regions are revealed via simulation method.

1. Introduction

Load frequency control (LFC) maintains the frequency of each control area and regulates the tie-line power flows between neighboring control areas [1, 2, 3]. In a deregulated environment, the power system consists of generation companies (Gencos), transmission companies (Transcos) and distribution companies (Discos) and is operated in an open assess policy [4, 5, 6]. The purpose of deregulation of power industry is to restructure the electric industry so that power production and distribution are competitive, but the delivery is still regulated, monopoly franchise business [7, 8]. Thus, the independent operator needs to develop a more reliable LFC service. On the other hand, the increasing penetration of intermittent renewable energy sources increases the complexity of the LFC in the deregulated environment [9].

Traditionally, the Gencos are designed to provide enough backup generation capacity to meet the peak load, which makes substantial backup capacity be idle for most hours within a year. Instead of providing enough generation capacity, demand side response (DSR) controls the load to balance the demand and the supply and becomes a promising smart grid technology, especially for

accommodating intermittent renewable generations [10, 11, 12]. Dynamic demand control (DDC) is one promising DSR technology which can provide the following two benefits in frequency control markets, providing an additional control [13] and reducing the spinning capacity [14]. DDC seeks to reduce the peak demands during period when the frequency stability is under threaten or electricity market prices are high. Market performance benefits refer to demand responses value in mitigating suppliers ability to exercise market power by raising electricity prices significantly above the production costs. Then market-wide financial benefit are the lower wholesale market prices because demand response averts the need to use the most costly-to-run power plants during periods of otherwise high demand, driving production costs and prices down for all wholesale electricity purchasers [15]. These savings may be passed onto most retail customers as bill savings.

Lots of efforts have been devoted to investigate the DDC for the LFC scheme [11, 12, 16]. Reference [11] investigates whether a degree of built-in frequency stability could be provided by incorporating DDC into certain consumer appliances. In [12], it introduces demand response control loop in the traditional single-area LFC scheme. This LFC with DSR model has the feature of optimal operation through optimal power between the supply side and the demand side. Conventionally, most DDC employs the thermostatically controlled appliances (TCAs), such as electric water heaters [17, 18], refrigerators [8, 11] and air conditioners [16, 19]. Compared with active energy storage device, for example, a battery or flywheel, the main advantage is that TCAs do not require expensive auxiliary equipment such as power converters to provide the service, while the disadvantage is that it is not energy source and cannot provide electricity to other end users when the grid power is lost [20, 21]. The potential of DSR for facilitating the integration of wind power in power system has been investigated [22, 23]. Most of those results have been carried out for the traditional LFC. To the best of authors' knowledge, the LFC with DDC in the deregulated environment has not received much efforts, while most DDC/DSR services are naturally expected to operate in the deregulated environment and competitive market.

Both the LFC scheme and the aggregation of DDC will use the communication channels to transmit the measurements and control commands, which will introduce time delays [24, 25]. Time delays will deteriorate the dynamic performance or even cause instability of the closed-loop system [26, 27, 28, 29, 30]. The maximum time delay which allows an LFC scheme embedded with controllers to retain stable is denoted as delay margin for stability analysis [2, 24]. The delay margin of the LFC scheme has been calculated and applied in the design of load frequency controller [27, 31]. The impact of the time delay on the DDC scheme has been investigated as well[11, 25]. However, to the best of authors' knowledge, the impact of multiple delays for the LFC with the DDC has not been investigated yet.

This paper targets to investigate the modeling and controller design of the LFC together with DDC, considering the impact of multiple delays in the control loops. Multiple time delays have been considered to formulate a time delay model of the LFC with DDC. A robust PID load frequency controller is designed to handle the multiple delays in the control loops, through the H_∞ performance analysis and the particle swarm optimization (PSO) searching algorithm, guaranteeing robustness to time delay and load disturbances. Case studies are based on a three area LFC schemes in deregulated environment. Effectiveness and robustness of the designed controller against to parameters uncertainties and delays are verified by simulation studies. Contribution of the DDC to frequency regulation has been compared, in terms of performance indices. Delay margins of the LFC scheme equipped with a PID-type controller have been obtained via trial-error simulation method. And the first and second delay stable region have been found, which reveals the fact that some large delays will stabilize the system again.

The rest of this paper is organized as follows. The time delay model of the deregulated multi-area LFC with DDC is obtained in Section II. Section III develops a method to design a robust PID controller. In section IV, case studies on a three-area deregulated LFC system with DDC are presented. Conclusions are drawn in Section V.

2. Time Delay Model of LFC with DDC

The model of power system with N frequency control areas in deregulated environment is discussed in this section. Figure 1 shows the control diagram of the i-th control area, in which the deregulated multi-area LFC scheme with n Gencos and m Discos, discussed in [27], and the DDC part are included. τ_{1i} and τ_{2i} are the communication delay in LFC control loop and DDC control loop, respectively. The communication delay τ_{ji} is represented by $e^{-s\tau_{ji}}$ in Figure 1. The following gives the model of LFC part, the model of the DDC part, and the state-space model of the whole closed-loop system.

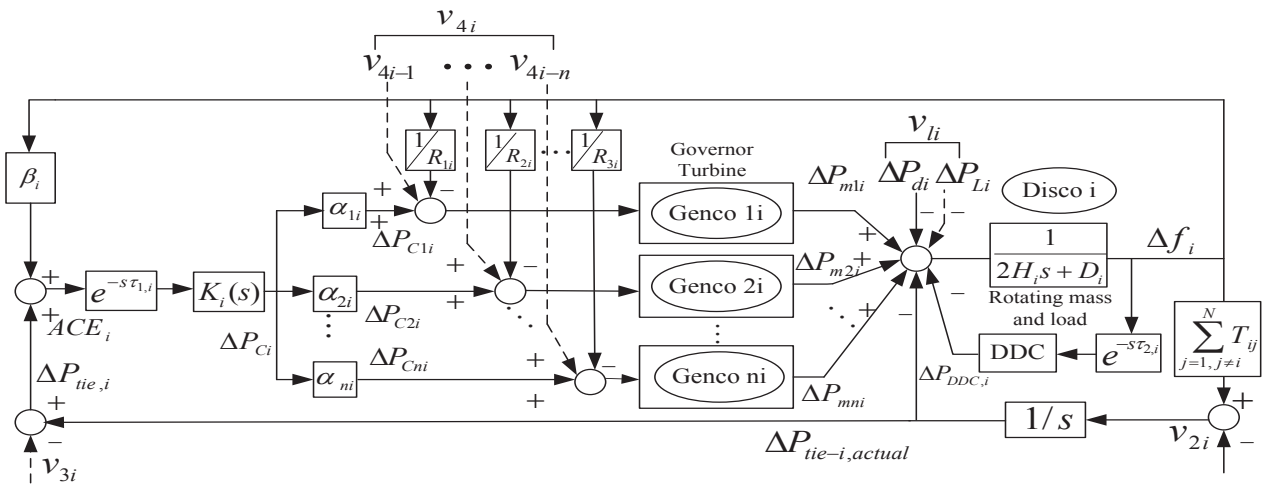

Fig. 1. *Time delay model of the ith control area of the multi-area deregulated LFC with DDC power system*

2.1. Model of Deregulated Multi-area LFC

Without loss of generality, all generators are assumed to equip with non-reheat turbine. The details model of deregulated multi-area LFC scheme including N control areas with n Gencos and m Discos in each area has been given in our previous work [27]. Here, we just recall some important parts strongly linked to following sections.

For a modern power system under deregulated environment, each Genco can contract with various Discos located in or out of the area this Genco belonging to. Those bilateral contracts are visualized by an augmented generation participation matrix (AGPM) [2]:

$$\mathrm{AGPM} = \begin{bmatrix} AGPM_{11} & \cdots & AGPM_{1N} \\ \vdots & \ddots & \vdots \\ AGPM_{N1} & \cdots & AGPM_{NN} \end{bmatrix} \tag{1}$$

where

$$\mathrm{AGPM_{ij}} = \begin{bmatrix} gpf_{s_i+1,z_j+1} & \cdots & gpf_{s_i+1,z_j+m} \\ \vdots & \ddots & \vdots \\ gpf_{s_i+n,z_j+1} & \cdots & gpf_{s_i+n,z_j+m} \end{bmatrix} \tag{2}$$

$s_i = n(i-1), z_j = m(j-1)$. The $\mathrm{gpf_{ij}}$ denotes the 'generation participation factor' of the Genco i in the total load following requirement of the Disco j based on the possible contracts. As there are many Gencos in each area, the relationship of $\mathrm{gpf_{ij}}$ is $\sum_{i=1}^{n} gpf_{ij} = 1$.

In Figure 1, the dotted line represents the new load demand signals corresponding to the possible contracts. They can be treated as additional disturbances of the traditional LFC scheme as follows [32]:

$$\upsilon_{1i} = \Delta P_{Li} + \Delta P_{di} = \sum_{j=1}^{m} \Delta P_{Lj-i} + \sum_{j=1}^{m} \Delta P_{ULj-i} \tag{3}$$

$$\upsilon_{3i} = \sum_{k=1,k\neq i}^{N} \Delta P_{tie,ik,sch} \tag{4}$$

$$\Delta P_{tie,ik,sch} = \sum_{j=1}^{n}\sum_{t=1}^{m} gpf_{s_i+j,z_k+t}\Delta P_{Lt-k} - \sum_{j=1}^{n}\sum_{t=1}^{m} gpf_{s_k+j,z_i+t}\Delta P_{Lt-i} \tag{5}$$

$$\Delta P_{tie-i} = \Delta P_{tie-i,actual} - \upsilon_{3i} \tag{6}$$

$$\upsilon_{4i}^{T} = \left[\upsilon_{4i,1} \cdots \upsilon_{4i,k} \cdots \upsilon_{4i,n}\right],\ \upsilon_{4i,k} = \sum_{j=1}^{N}\sum_{t=1}^{m} gpf_{s_i+k,z_j+t}\Delta P_{Lt-j} \tag{7}$$

$$\Delta P_{mk-i} = \upsilon_{4i,k} + \alpha_{ki}(\sum_{j=1}^{m} \Delta P_{UL_{j-i}} + \Delta P_{ddc,i}) \tag{8}$$

where ΔP_{Li} and ΔP_{di} are the total contracted and un-contracted demand in area i, respectively; ΔP_{Lj-i} and ΔP_{ULj-i} are the contracted and un-contracted demand of Disco j in area i, respectively; $\Delta P_{tie,ik,sch}$ and $\Delta P_{m,k-i}$ are the scheduled tie-line power exchange between area i and area k and the desired total power generation of Genco k in area i.

In multi-area LFC system, the area control error (ACE) is defined as

$$ACE_i = \beta_i \Delta f_i + \Delta P_{tie,i} \tag{9}$$

where Δf_i and β_i are deviation of frequency and frequency bias factor in area i, respectively.

Using ACE as the input of LFC, a PID controller is designed as

$$u_i(t) = -K_{Pi}ACE_i - K_{Ii}\int ACE_i dt - K_{Di}\frac{d}{dt}ACE_i \tag{10}$$

where $K_i = [K_{Pi}\ \ K_{Ii}\ \ K_{Di}]$ stands for proportional, integral and derivative gains, respectively. The $K_i(s)$ in Figure 1 stands for PID controller used in LFC system.

2.2. Model of Dynamic Demand Control

Domestic electric appliances can be classified into five different groups based on their characteristics[34], in which the thermostatically controlled load (such as air conditioners, refrigerators and water heaters) and domestic wet-appliances with induction motors or heaters (for example washing machines and dryers) can be used as controllable load for frequency regulation, since they are relevant directly to the frequency derivation. In this paper, a typical thermostatically controlled load, air conditioner, is considered as the DDC loads, in which the controllable loads participate in the DDC scheme by adjusting their usage of electricity based on the deviation of the system frequency [33].

The frequency dependent characteristic of thermostatical load can be expressed as:

$$\Delta P_{\mathrm{ddc,i}} = \Delta P_{LC,i} + D_{ac,i}\Delta\omega_i \tag{11}$$

where $\Delta P_{LC,i}$ is the load change based on different load characteristic and $D_{ac,i}$ is damping coefficient.

Based on the DDC model (11), $\Delta P_{LC,i}$ depends on the characteristic of the air conditioner and the set point ($\Delta T_{st,i}$) of a smart thermostat, and can be represented as follows:

$$\Delta P_{LC,i} = (m_i c_{p,i}\Delta T_{st,i})/EER \tag{12}$$

where m_i is the mass of air flow, $c_{p,i}$ is the specific heat capacity of the air, and EER is the energy efficiency ratio (EER) defined as the ratio of the capacity output to electricity input of an air conditioner [36].

The smart thermostat is usually controlled via an integral controller using the frequency deviation (Δf_i) from the ith control area as the input and the temperature set-point as the output. The $\Delta T_{st,i}$ is given as

$$\Delta T_{st,i} = k\int \alpha\Delta f_i dt \tag{13}$$

where k is the gain factor in the smart thermostat and given as 10 and α is a coefficient and given as 0.5Rs/Hz. The temperature set-point is bounded and varies based on the weather condition and different time interval in a day. In this paper, these variations are ignored and the thermostat set-point is simply bounded as $[24°C, 29°C]$.

Finally, the load model of air conditioner is given as:

$$\begin{aligned}\Delta P_{\mathrm{ddc,i}} &= (m_i c_{p,i} K\int 0.5\Delta f_i dt)/EER + D_{ac,i}2\pi\Delta f_i \\ &= 0.5k_i\int \Delta f_i dt + 2\pi D_{ac,i}\Delta f_i\end{aligned} \tag{14}$$

where $k_i = \frac{m_i c_{p,i} k}{EER}$ is the combined integral gain.

Due to the small capacity of an individual household load, it is necessary to aggregate a number of small domestic loads into a relative large and lumped DDC load to participate the LFC scheme [35]. The scheme of DDC business model includes smart meters, smart sockets which communicated through a home-area-network and a smart load controller [34]. Aggregation DDC model is simplified as a linearly amplified of model (14) plus a time delay and this delay will be combined with the delay of transmitting Δf_i and represented by $\tau_{2,i}$.

2.3. Closed-loop State Space Model of LFC with DDC

When the DDC is included, based on the new power energy balance equation, the dynamic equation of the frequency deviation will be changed as follows

$$\frac{d}{dt}\Delta f_i = \frac{1}{2H_i}[\sum_{j=1}^{n}\Delta P_{mji} - (\Delta P_{di} + \Delta P_{Li}) - \Delta P_{tie-i,actual} - \Delta P_{ddc,i} - D_i\Delta f_i] \tag{15}$$

Based on the transfer function of DDC (equation (14)), dynamic model of DDC considering the time delay can be expressed as following:

$$\begin{aligned}\frac{d}{dt}\Delta P_{ddc,i} =& (0.5K_I - D_{ac,i}\frac{2\pi D_i}{2H_i})\Delta f_i(t-\tau_{2,i}) + \frac{2\pi D_{ac,i}}{2H_i}[\sum_{j=1}^{n}\Delta P_{mji}(t-\tau_{2,i}) \\ &- \frac{2\pi D_{ac,i}}{2H_i}\Delta P_{tie-i,actual}(t-\tau_{2,i}) - \frac{2\pi D_{ac,i}}{2H_i}\Delta P_{ddc,i}(t-\tau_{2,i}) \\ &- \frac{2\pi D_{ac,i}}{2H_i}(\Delta P_{di} + \Delta P_{Li})\end{aligned} \tag{16}$$

In [27], it presents the multi-area deregulated LFC system in state-space. Based on this reference and dynamic equations (15) and (16), the state-space model of multi-area LFC with DDC in deregulated environment can be obtained as:

$$\begin{cases}\dot{x}_i(t) &= A_i x_i(t) + A_{di}x_i(t-\tau_{2i}) + B_i u_i(t-\tau_{1i}) + F_i\nu_i \\ y_i(t) &= C_i x_i(t) + E_i\nu_i\end{cases} \tag{17}$$

where

$x_i^T = [\Delta f_i, \Delta P_{\mathrm{tie}-i}, \Delta P_{\mathrm{m}1i}, \cdots, \Delta P_{\mathrm{m}ni}, \Delta P_{\mathrm{g}1i}, \cdots, \Delta P_{\mathrm{g}ni}, \Delta P_{ddc,i}]$

$y_i = ACE_i, \nu_i^T = [\nu_{1i}, \nu_{2i}, \nu_{3i}, \nu_{4i}]$

$$A_i = \begin{bmatrix} A_{11i} & A_{12i} & 0_{2\times n} & A_{14i} \\ 0_{n\times 2} & A_{22i} & A_{23i} & 0_{n\times 1} \\ A_{31i} & 0_{n\times n} & A_{33i} & 0_{n\times 1} \\ 0_{1\times 2} & 0_{1\times n} & 0_{1\times n} & 0 \end{bmatrix}, A_{di} = \begin{bmatrix} 0_{2\times 2} & 0_{2\times n} & 0_{2\times n} & 0 \\ 0_{n\times 2} & 0_{n\times n} & 0_{n\times n} & 0 \\ 0_{n\times 2} & 0_{n\times n} & 0_{n\times n} & 0 \\ A_{41di} & A_{42di} & 0_{1\times n} & -\frac{2\pi D_{ac,i}}{2H_i} \end{bmatrix}, B_i = \begin{bmatrix} 0_{2\times 1} \\ 0_{n\times 1} \\ B_{3i} \\ 0 \end{bmatrix}$$

$$F_i = \begin{bmatrix} F_{11i} & F_{12i} & 0_{2\times 1} & 0_{2\times n} \\ 0_{n\times 1} & 0_{n\times 1} & 0_{n\times 1} & 0_{n\times n} \\ 0_{n\times 1} & 0_{n\times 1} & 0_{n\times 1} & F_{33i} \\ -\frac{2\pi D_{ac,i}}{2H_i} & 0 & 0 & 0 \end{bmatrix}, C_i = \begin{bmatrix} \beta_i & 1 & 0_{1\times 2n} & 0 \end{bmatrix}, E_i = \begin{bmatrix} 0 & 0 & -1 & 0_{1\times n} \end{bmatrix}^T$$

$$A_{11i} = \begin{bmatrix} -\frac{D_i}{2H_i} & -\frac{1}{2H_i} \\ 2\pi\sum_{j=1,j\neq i}^{N} T_{ij} & 0 \end{bmatrix}, A_{12i} = \begin{bmatrix} \frac{1}{2H_i} & \cdots & \frac{1}{2H_i} \\ 0 & \cdots & 0 \end{bmatrix}, A_{14i} = \begin{bmatrix} -\frac{1}{2H_i} \\ 0 \end{bmatrix}$$

$$A_{22i} = -A_{23i} = \mathrm{diag}\{ -\tfrac{1}{T_{\mathrm{t}1i}}, \cdots, -\tfrac{1}{T_{\mathrm{t}ni,}} \}, A_{31i} = \begin{bmatrix} \frac{-1}{T_{\mathrm{g}1i}R_{1i}} & \cdots & \frac{-1}{T_{\mathrm{g}ni}R_{ni}} \\ 0 & \cdots & 0 \end{bmatrix}^T$$

$$A_{33i} = -F_{33i} = \mathrm{diag}\{ \tfrac{-1}{T_{\mathrm{g}1i}}, \cdots, \tfrac{-1}{T_{\mathrm{g}ni}} \}, A_{41di} = \begin{bmatrix} 0.5K_I - \frac{2D_{ac,i}\pi D_i}{2H_i} & -\frac{2\pi D_{ac,i}}{2H_i} \end{bmatrix}$$

$$A_{42di} = \begin{bmatrix} \frac{2\pi D_{ac,i}}{2H_i} & \cdots & \frac{2\pi D_{ac,i}}{2H_i} \end{bmatrix}, B_{3i} = \begin{bmatrix} \frac{\alpha_{1i}}{T_{\mathrm{g}1i}} & \cdots & \frac{\alpha_{ni}}{T_{\mathrm{g}ni}} \end{bmatrix}^T, F_{11i} = \begin{bmatrix} \frac{-1}{2H_i} & 0 \end{bmatrix}^T, F_{12i} = \begin{bmatrix} 0 & -2\pi \end{bmatrix}^T$$

$$F_{33i} = \mathrm{diag}\{ \tfrac{1}{T_{\mathrm{g}1i}}, \cdots, \tfrac{1}{T_{\mathrm{g}ni}} \}$$

The ΔP_{gki} is valve position. The $2H_i$, D_i, T_{gki}, T_{tki} and R_{ki} are the moment of inertia of generator unit, generator unit damping coefficient, time constant of the governor, time constant of the turbine and speed drop, respectively. The α_{ki} is participation factor. $v_i, i = 1, 2, 3, 4$ are the disturbances of area i caused by the possible contracts and load changing (Refer to [26] for more details).

To obtain the state space model of the closed-loop system, the PID-type control problem should be transformed into a static output feedback control problem. Define the following virtual vectors $\bar{x}_i = [x_i^T \ \int y_i^T]^T$ and $\bar{y}_i = [y_i \ \int y_i dt \ (d/dt)y_i]^T$, the closed-loop system can be rewritten as

$$\begin{cases} \dot{\bar{x}}_i(t) &= \bar{A}_i\bar{x}_i(t) + \bar{A}_{di}\bar{x}_i(t-\tau_{2i}) - \bar{B}_iK_i\bar{C}_ix(t-\tau_{1i}) + (\bar{F}_i - \bar{B}_iK_i\bar{D}_i)\nu_i \\ \bar{y}_i(t) &= \bar{C}_i\bar{x}_i(t) + \bar{D}_i\nu_i \end{cases} \tag{18}$$

where

$$\bar{A}_i = \begin{bmatrix} A_i & 0 \\ C_i & 0 \end{bmatrix}, \bar{A}_{di} = \begin{bmatrix} A_{di} & 0 \\ 0 & 0 \end{bmatrix}, \bar{B}_i = \begin{bmatrix} B_i \\ 0 \end{bmatrix}, \bar{C}_i = \begin{bmatrix} C_i & 0 \\ 0 & 1 \\ C_iA_i & 0 \end{bmatrix}, \bar{F}_i = \begin{bmatrix} F_i \\ 0 \end{bmatrix}, \bar{E}_i = \begin{bmatrix} E_i \\ 0 \\ C_iF_i \end{bmatrix}$$

$$K_i = \begin{bmatrix} K_{Pi} & K_{Ii} & K_{Di} \end{bmatrix}$$

3. Robust Controller Design

This section develops a method to design a robust PID controller through the H_∞ performance analysis and the PSO searching algorithm. Firstly, a performance criterion is derived to construct the relationships among the delay, robust performance index, and PID gains. Then, the tuning of the PID gains is transformed into an optimization problem solved by PSO algorithm.

3.1. A performance criterion

By assuming the time delays in LFC and DDC loops be identical and defining the concerned output $z(t) = [\Delta f_i, \Delta P_{tie,i}]^T$, the closed-loop system for control areas shown in (18) can be described by the following general form:

$$\begin{cases} \dot{x}(t) &= Ax(t) + (A_d - BKC_y)x(t-h) + (B_\omega - BKD)\omega(t) \\ z(t) &= C_zx(t) \end{cases} \tag{19}$$

where $x(t) = \bar{x}_i(t)$, $h = \tau_{1i} = \tau_{2i}$, $\omega(t) = v_i(t)$, $B_\omega = \bar{F}_i$, $C_y = \bar{C}_i$, and $C_z = \begin{bmatrix} I_{2\times2}, 0_{2\times(2+2n)} \end{bmatrix}$.

The following criterion is derived by using the Lyapunov-Krasovskii functional (LKF) method and the Jensen integral inequality.

Theorem 1. For given the delay h, the H_∞ performance index γ, and the controller gains $K = [K_P, K_I, K_D]$, the closed-loop system (19) is stable and has performance index, γ, against a non-zero disturbance for any delays smaller than h, if there exist symmetric matrices P, Q, and R, such that the following linear matrix inequalities hold

$$P > 0, Q > 0, R > 0 \tag{20}$$

$$\begin{aligned} \Phi = e_1^TPe_s + e_s^TPe_1 + e_1^T(Q + C_z^TC_z)e_1 - e_2^TQe_2 + h^2e_s^TRe_s - \gamma^2e_3^Te_3 \\ -(e_1-e_2)^TR(e_1-e_2) < 0 \end{aligned} \tag{21}$$

where $e_s = \begin{bmatrix} A, \ A_d - BKC_y, \ B_w - BKD \end{bmatrix}$, $e_1 = \begin{bmatrix} I, \ 0, \ 0 \end{bmatrix}$, $e_2 = \begin{bmatrix} 0, \ I, \ 0 \end{bmatrix}$, and $e_3 = \begin{bmatrix} 0, \ 0, \ I \end{bmatrix}$.

Proof: Choose an LKF candidate as follows:

$$V(t) = x^T(t)Px(t) + \int_{t-h}^{t} x^T(s)Qx(s)ds + h\int_{-h}^{0}\int_{t+\theta}^{t} \dot{x}^T(s)R\dot{x}(s)dsd\theta \tag{22}$$

where $P > 0$, $Q > 0$, and $R > 0$, which indicates $V(t) > 0$. Calculating the derivative of LKF and using Jensen integral inequality yield

$$\begin{aligned}\dot{V}(t) &= 2x^T(t)P\dot{x}(t) + x^T(t)Qx(t) - x^T(t-h)Qx(t-h) + h^2\dot{x}^T(t)R\dot{x}(t) - h\int_{t-h}^{t}\dot{x}^T(s)R\dot{x}(s)ds \\ &\leq 2x^T(t)P\dot{x}(t) + x^T(t)Qx(t) - x^T(t-h)Qx(t-h) \\ &\quad + h^2\dot{x}^T(t)R\dot{x}(t) - (x(t)-x(t-h))^T R(x(t)-x(t-h)) \end{aligned} \tag{23}$$

where $\zeta(t) = \left[\ x(t),\ x(t-h),\ \omega(t)\ \right]$. It follows from LMI (21) that

$$\dot{V}(t) + z^T(t)z(t) - \gamma^2\omega^T(t)\omega(t) < \zeta^T(t)\Phi\zeta(t) \tag{24}$$

where Φ is defined in (21). Then, the following holds

$$\Phi < 0 \Rightarrow \int_0^{\infty}[z^T(s)z(s) - \gamma^2\omega^T(s)\omega(s)]ds \leq 0 \tag{25}$$

Therefore, the holding of LMI (21) leads to $\frac{\|z(t)\|}{\|\omega(t)\|} \leq \gamma$, which means the system is stable and has a H_∞ performance index, γ. This completes the proof.

3.2. PID Gain Tuning via the PSO Algorithm

Theorem 1 gives the relationships among the delay h, the H_∞ performance index γ, and the PID gains K. As discussed in [26], for fixed delay h and the controller gain K, one can find the minimal value of the performance index γ_{min} through the conditions of Theorem 1. That is, the minimal value γ_{min} is a function of the delay h and the controller gains K, as described as follows

$$\gamma_{min} = f(h, K_P, K_I, K_D) \tag{26}$$

How to calculate the minimal value, γ_{min}, for fixed delay bound h and the controller gains K can be found in [26] and is omitted here due to page limitation.

To provide the optimal robust performance against to the delays and the disturbances, control gains tuning can be transformed to the following optimization problem:

$$\begin{aligned} Minimize: &\quad \gamma_{min} = f(h, K_P, K_I, K_D) && (27)\\ subjectto: &\quad K_{Pmin} \leq K_P \leq K_{Pmax} && (28)\\ &\quad K_{Imin} \leq K_I \leq K_{Imax} && (29)\\ &\quad K_{Dmin} \leq K_D \leq K_{Dmax} && (30)\end{aligned}$$

The above optimization problem can be solved by various algorithms. This paper chooses the PSO searching algorithm as it is a meta-heuristic algorithm and has been widely used due to its decent performance in numerical optimization [37]. The details are omitted here since the PSO is standard algorithm and can be easily achieved by Matlab (The MathWorks, Natick, Massachusetts, USA).

4. Case Studies

Case studies are based on a deregulated three-area LFC system, as shown in Figure 2. Each control area consists of two Gencos, two Discos, and one DDC. The related parameters are given in [16, 32] and listed in Table 1. The robust PID controllers for each control area are designed based on the linear time-delay model given in Section 2 and the method proposed in Section 3, and their effectiveness, robustness against to parameter uncertainties and time delays as well, is verified via simulation studies completed based on Figure 2 with some nonlinearities, including the generation rate constraint (GRC) and the dead bands. All calculations and simulations are carried out by using Matlab 7.10.0 (R2010a) running on a PC with 2.80-GHz Intel Core i7 CPU, 8GB RAM, and Windows 7 64-bit Ultimate.

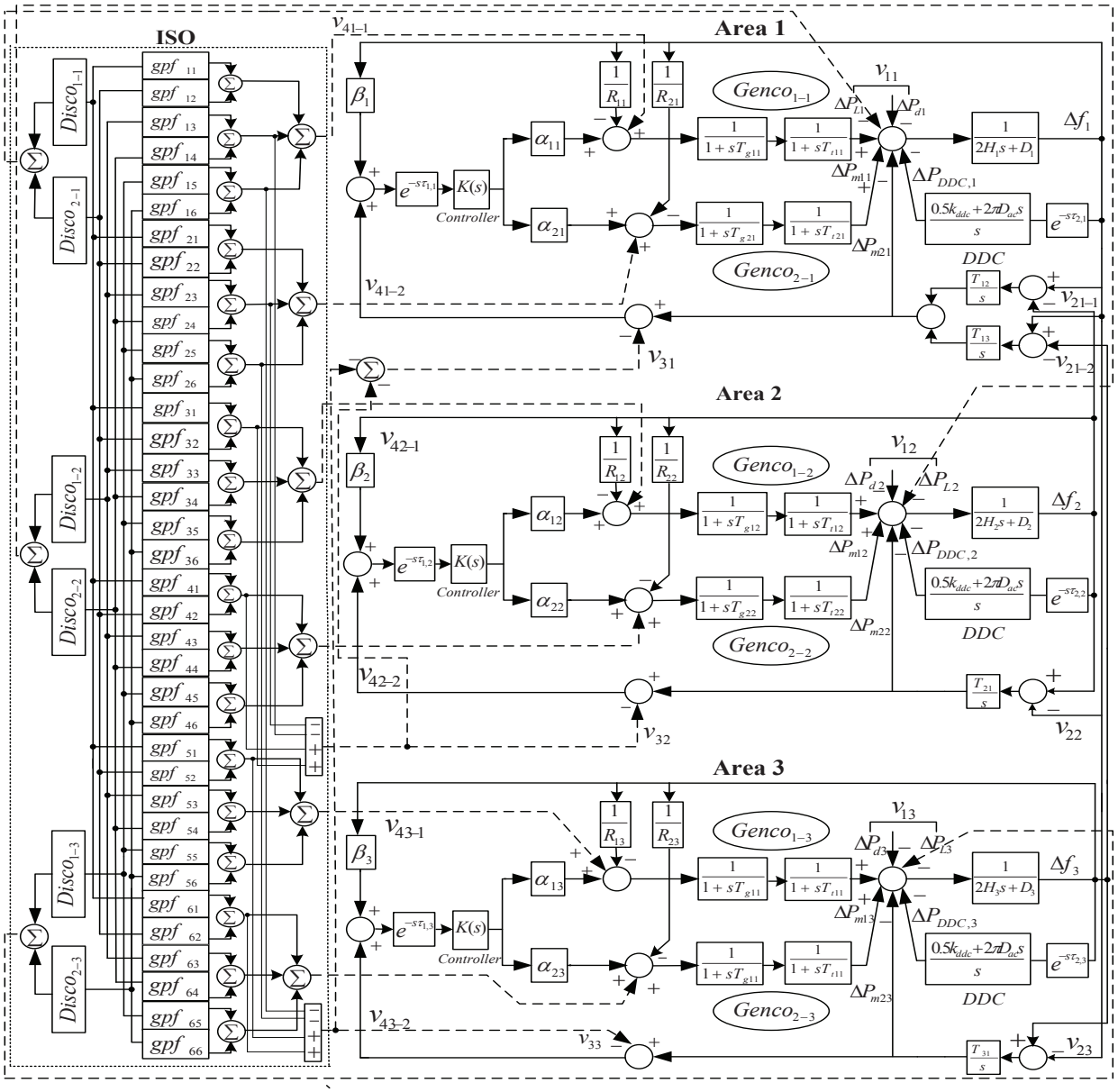

Fig. 2. *Three-area deregulated LFC test system*

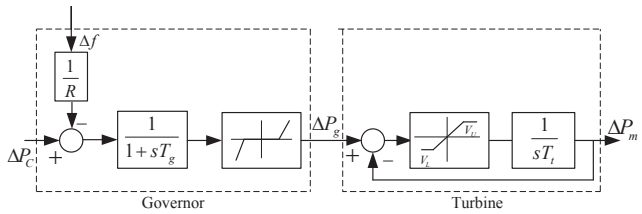

Fig. 3. *Non-reheat generator unit model with GRC and dead band*

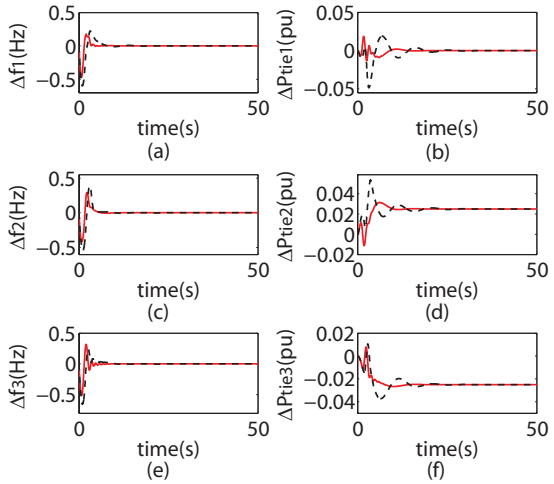

Fig. 4. *Frequency deviation and tie-line power exchange of the three-area power system: Solid (with DDC), Dashed (without DDC). (a) Frequency deviation in area 1. (b) Tie-line power exchange in area 1. (c) Frequency deviation in area 2. (d) Tie-line power exchange in area 2. (e) Frequency deviation in area 3. (f) Tie-line power exchange in area 3.*

4.1. Controller design and its verification

1) Control design: To simplify the design procedure, the time delays of three areas are preset as the same value, 0.2 s. The search regions for PID gains are set to be [-1,1]. By using the robust performance index (RPI)-based objective function calculated by the method in [26] and the standard PSO-based search method, all achieved through Matlab platform, the PID gains for three areas are obtained as follows:

$$K_1 = [0.79133, -0.56537, -0.19693]$$
$$K_2 = [-0.05968, -0.96936, -0.26727]$$
$$K_3 = [-0.13721, -0.84983, -0.41357]$$

2) Simulation verification: During the construction of simulation platform of the concerned three-area LFC, the linear model of governor and turbine in Figure 1 is replaced by the nonlinear model shown in Figure 3, in which the GRC is assumed to be 0.1 pu/min and the dead band range is assumed to be 0.036 Hz [2].

The communication time delays in LFC and DDC loops are given as 0.2s. The power supply

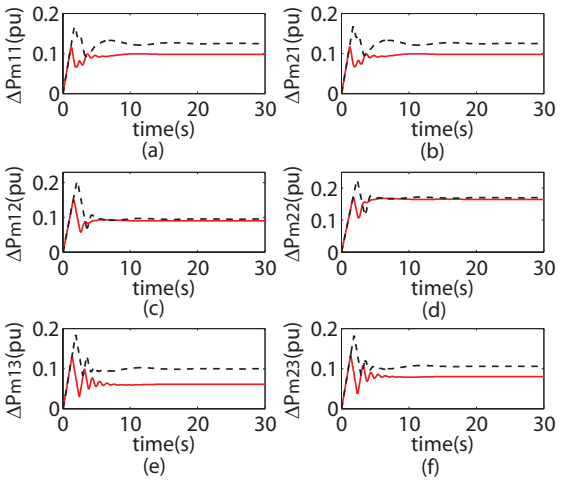

Fig. 5. *Response of six Gencos mechanical power of the three-area power system: Solid (with DDC), Dashed (without DDC). (a) Mechanical power of Genco1 in area 1. (b) Mechanical power of Genco2 in area 1. (c) Mechanical power of Genco1 in area 2. (d) Mechanical power of Genco2 in area 2. (e) Mechanical power of Genco1 in area 3. (f) Mechanical power of Genco2 in area 3.*

Table 1 The parameters of the concerned system

	Gencos							Areas				Areas		
	1-1	2-1	1-2	2-2	1-3	2-3		1	2	3		1	2	3
T_{T}	0.32	0.30	0.30	0.32	0.31	0.34	H	0.0833	0.1042	0.0800	c_p	1.01	1.01	1.01
T_{G}	0.06	0.08	0.06	0.07	0.08	0.06	D	0.0083	0.0083	0.0080	m	0.25	0.05	0.15
R	2.4	2.5	2.5	2.7	2.8	2.4	β	0.4250	0.3966	0.3522	k	8	15	10
α	0.5	0.5	0.5	0.5	0.6	0.4	$T_{12} = 0.0389, T_{13} = 0.0337,$ $T_{23} = 0$				$D_{ac,i}$	0.025	0.015	0.01

contract among all Discos and Gencos related follows the following AGPM [32]:

$$\mathrm{AGPM} = \begin{bmatrix} 0.25 & 0 & 0.25 & 0 & 0.5 & 0 \\ 0.5 & 0.25 & 0 & 0.25 & 0 & 0 \\ 0 & 0.5 & 0.25 & 0 & 0 & 0 \\ 0.25 & 0 & 0.5 & 0.75 & 0 & 0 \\ 0 & 0.25 & 0 & 0 & 0.5 & 0 \\ 0 & 0 & 0 & 0 & 0 & 1 \end{bmatrix} \tag{31}$$

Assume that a step load of 0.1 pu is demanded by each Disco in the areas, and Disco 1 in area 1 and area 2, and Disco 2 in area 3 demand 0.05 pu, 0.04 pu, and 0.03 pu as un-contracted loads, i.e., $\Delta P_{Lj-i} = 0.1pu, i = 1, 2, 3; j = 1, 2$; $\Delta P_{UL1-1} = 0.05pu$; $\Delta P_{UL1-2} = 0.04pu$; and $\Delta P_{UL1-3} = 0.03pu$.

The responses of system are shown in Figure 4. The frequency deviation and tie-line power exchange are quickly convergent to schedule values, which means the designed PID controller is effective. Using equation (5), the value of tie-line power exchange is calculated and given as follows: $\Delta P_{tie1} = 0$ pu MW, $\Delta P_{tie2} = 0.025$ pu MW and $\Delta P_{tie3} = -0.025$ pu MW. Moreover, it can be found that the LFC with DDC can provide better dynamic performances, shorter settling time and smaller overshoot, compared with the one without DDC, which shows that the introducing

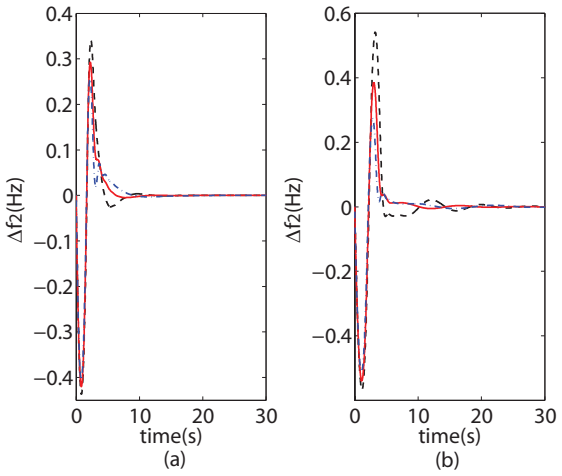

Fig. 6. *Frequency deviation of area 2 under system parameters variation: Solid (normal value), Dashed (increased 25%), Dashdotted (decreased 25%). (a) LFC with DDC. (b) LFC without DDC.*

of the DDC enhances the transient response of frequency regulation. Mechanical power changing of Gencos in LFC with DDC and LFC without DDC is displayed in Figure 5. When the DDC part is participated in LFC deregulated power system, the mechanical power change of each Genco is smaller than LFC without DDC. The value of power deviation from each DDC can be obtained via solving the equilibrium point from the state space of equation (17) as follows: $\Delta P_{\mathrm{ddc},1} = 0.054$ pu MW, $\Delta P_{\mathrm{ddc},2} = 0.010$ pu MW and $\Delta P_{\mathrm{ddc},3} = 0.064$ pu MW. Then using equation (8), the value of mechanical power change of each Genco in LFC with DDC is calculated and given as follows: $\Delta P_{\mathrm{m}11} = \Delta P_{\mathrm{m}21} = 0.098$ pu MW, $\Delta P_{\mathrm{m}12} = 0.090$ pu MW, $\Delta P_{\mathrm{m}22} = 0.165$ pu MW, $\Delta P_{\mathrm{m}13} = 0.061$ pu MW and $\Delta P_{\mathrm{m}23} = 0.080$ pu MW. The simulation results reveal that the LFC scheme with the DDC can drive the power system in stable faster and have smaller fluctuation.

4.2. Robustness against to parameters uncertainties

The PID controller aforementioned is tuned for the nominal systems parameters. However, in reality, there exist uncertainties in the system parameters due to measurement errors etc., as well in the controller gains during the implementation procedure. Therefore, the robustness against those parameters uncertainties also is tested. To indicate the dynamic performances, the following two indexes, the integral of the time multiplied absolute value of the error (ITAE) and integral of the time multiplied square of the error (ITSE), with respect to ACE (ACE_i) are defined:

$$\mathrm{ITAE} = \int_0^{\mathrm{t}} \mathrm{t}(|\mathrm{ACE}_1| + |\mathrm{ACE}_2| + |\mathrm{ACE}_3|)|)\mathrm{dt} \tag{32}$$

$$\mathrm{ITSE} = \int_0^{\mathrm{t}} \mathrm{t}(\mathrm{ACE}_1^2 + \mathrm{ACE}_2^2 + \mathrm{ACE}_3^2)\mathrm{dt} \tag{33}$$

Two cases, including uncertainties in system parameters (within $\pm 25\%$), and uncertainties in both system parameters and controller gains (within $\pm 25\%$), are simulated. Note that other operation conditions (time delays, load changes) are the same to ones given in Section 4.1. When only the system parameter uncertainties are considered, the values of ITAE and ITSE for some typical uncertainties are given in Table 2. Also, Figure 6 shows the frequency deviation of control area 2 when system parameters are in normal value, 125% and 75% of normal value, respectively. When the uncertainties exist in both system parameters and controller gains are in normal value,

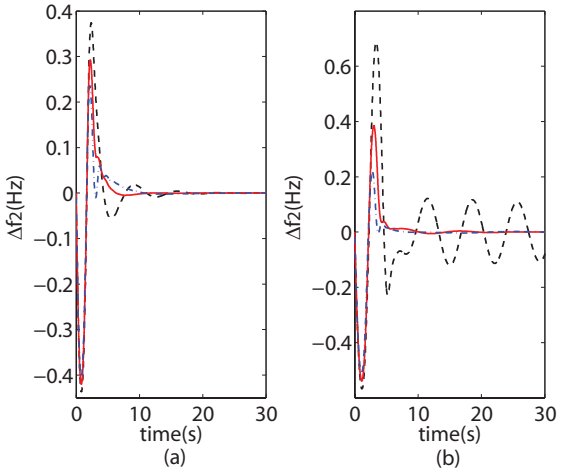

Fig. 7. *Frequency deviation of area 2 for system and controller uncertainties: Solid (normal value), Dashed (increased 25%), Dashdotted (decreased 25%) (a) LFC with DDC. (b) LFC without DDC.*

125% and 75% of normal value, the frequency deviation of control area 2 are shown in Figure 7, respectively.

From Table 2 and Figures 6 and 7, it can be found that the designed PID controller stabilizes the LFC system even the uncertainties exist, which shows the robustness of controller against to parameter uncertainties. Meanwhile, it can be found that the introducing of DDC can stabilize LFC system more quickly with smaller fluctuation and provide better performance indexes. Furthermore, from Figure 7(b), which shows that, when both system and controller parameters increase 25%, the LFC without DDC can not maintain stable while the LFC with DDC is still stable, it is concluded that the DDC can not only improve the transient responses of system but also provide better robustness against to parameter uncertainties.

Table 2 Dynamic performance indices (ITAE and ITSE)

Parameter change (%)	Parameter Change				Controller Parameter Change			
	without DDC		with DDC		without DDC		with DDC	
	ITAE	ITSE	ITAE	ITSE	ITAE	ITSE	ITAE	ITSE
0%	1.74	0.11	4.64	0.33	1.74	0.11	4.64	0.33
+5	1.90	0.13	4.86	0.40	1.81	0.12	5.13	0.35
-5	1.63	0.10	4.59	0.28	1.68	0.11	4.26	0.31
+10	2.11	0.15	5.42	0.49	1.90	0.12	5.81	0.37
-10	1.56	0.09	4.59	0.24	1.63	0.11	3.96	0.30
+15	2.36	0.18	6.54	0.62	2.01	0.12	6.74	0.40
-15	1.53	0.08	4.67	0.21	1.59	0.11	3.71	0.28
+20	2.66	0.21	8.50	0.81	2.14	0.13	8.07	0.44
-20	1.55	0.07	4.82	0.18	1.57	0.11	3.50	0.27
+25	3.02	0.26	11.56	1.10	2.30	0.13	10.06	0.49
-25	1.65	0.06	5.01	0.15	1.54	0.11	3.31	0.26

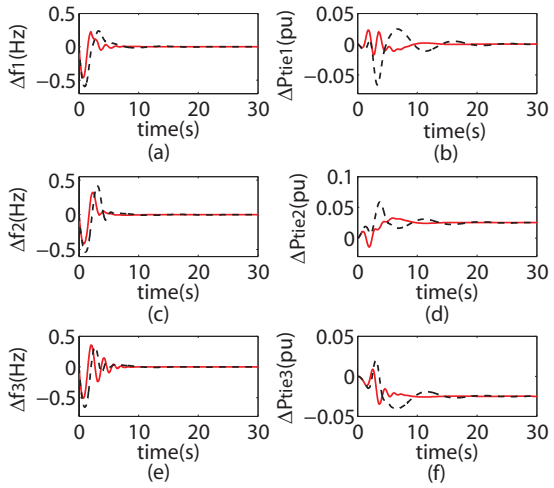

Fig. 8. *Deviation of frequency and and tie line power exchange of the three-area power system with time-varying delay: Solid (with DDC), Dashed (without DDC). (a) Frequency deviation in area 1. (b) Tie-line power exchange in area 1. (c) Frequency deviation in area 2. (d) Tie-line power exchange in area 2. (e) Frequency deviation in area 3. (f) Tie-line power exchange in area 3.*

4.3. Robustness against to time delays

The PID controller designed in Section 4.1 is tuned by setting all delays to be constant, 0.2s. However, in reality, there usually exist time-varying delays and the delays for different areas and loops are not identical. Therefore, this subsection tests the robustness against to time-varying/random delays and finds the delay margin for different areas.

1) Random delays: The different random delays within the range [0s,0.4s] are added into the LFC and DDC loops of three areas. The responses of the LFC system are given in Figure 8. Although the upper bound of the random delay (0.4s) is bigger than the delay (0.2s) for control design in Section 4.1, the frequency deviation is still quickly back to zero and power exchanges back to schedule value with short setting time, which shows the robustness of the designed PID controller against to time-vary and random delays. Moreover, the LFC with DDC has better dynamic performance.

2) Multiple delay stable regions: The contribution of the DDC to improve the dynamic performances of LFC systems has been revealed in the previous simulation results. During testing such contribution, an important factor needed to consider is the time delay. If the time delay is too big, the introducing of DDC may no contribution to improve the performance and even leads to instability phenomenon. The time delays in LFC loop of each area are assumed to be 0.3s. This part tests the admissible delay ranges, under which the LFC with DDC remains stable, by manual increasing the delay in the DDC loop step by step and observing the whole system stability. Figure 9 shows one example for area 2 under different time delays. The results are found and listed in Table 3. It is found that there are multiple delay stable regions, only two of them are given in this paper, defined as the first stability region (FSR) and the second stability region (SSR) respectively.

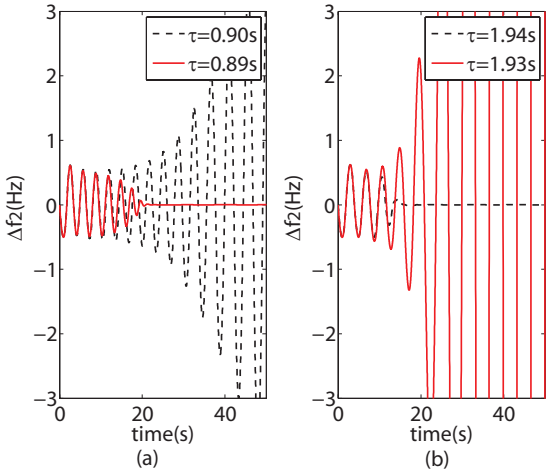

Fig. 9. *Frequency deviation of area 2 for different delay in DDC loop. (a) FSR. (b) SSR.*

Table 3 Delay stable regions for each area

Control Area	First stable Region (s)	Second Stable Region (s)
1	[0 3.15]	[5.70 11.10]
2	[0 0.89]	[1.94 11.50]
3	[0 0.48]	[1.87 11.00]

5. Conclusions

This paper has investigated a robust PID-type controller for LFC with DDC in a deregulated multi-area power system. A robust PID controller design method has been proposed, through the H_∞ performance analysis and the PSO searching algorithm, to design a PID load frequency controller providing the robustness to the load disturbances, the parameter uncertainties, and the multiple delays in the LFC loop and the DDC loop. Case studies are based on a deregulated three-area LFC system. Simulation results demonstrate that the effectiveness of the proposed PID controller, and robustness against parameter uncertainties and multiple time delays. It also shows that the LFC with DDC can provide better dynamic performance, in terms of performance index ITAE and ITSE. Moreover, delay margins of LFC with DDC are obtained via trial-and-error simulation method, and multiple stability regions have been found, which shows that large delay may re-stabilize the LFC system.

Future work will focus on theoretically investigating the multiple stability regions of LFC with multiple delays and also designs/synthesises of controller considering those delay regions.

Funding

This work was supported by National Natural Science Foundation of China under Grant No. 51428702 and the National Basic Research Program of China (973 Program) under Grant No. 2012CB215106.

6. References

[1] Ibraheem, Kumar, P., and Kothari, D. P., "Recent philosophies of automatic generation control strategies in power system," *IEEE Trans. Power Syst.*, Vol. 20, No. 1, pp. 346-357, February 2005.

[2] Bevrani, H., *Robust power system frequency control*, Berlin, Springer, 2009.

[3] Sahu, R. K., Panda, S., and Pradhan, P. C., "Design and analysis of hybrid firefly algorithm-pattern search based fuzzy PID controller for LFC of multi area power systems," *Int. J. Electr. Power Energy Syst.*, Vol. 69, pp. 200-212, July 2015.

[4] Panday, S. K., Mohanty, S. R., and Kishor, N., "A literature survey on load-frequency control for conventional and distribution generation power systems," *Renew. Sust. Energ. Rev.*, Vol. 25, pp. 318-334, September 2013.

[5] Bakken B. H., and Grande, O. S., "Automatic generation control in a deregulated power system," *IEEE Trans. Power Syst.*, Vol. 13, No. 4, pp. 1401-1406, November 1998.

[6] Arya, Y., and Kumar, N., "AGC of a multi-area multi-source hydrothermal power system interconnected via AC/DC parallel links under deregulated environment," *Int. J. Electr. Power Energy Syst.*, Vol. 75, pp. 127-138, February 2016.

[7] Abhyankar, A. R., and Khaparde, S. A., "Introduction to deregulation in power industry," *Indian institute of technology bombay*, pp. 1-28, 2003.

[8] Angeli, D., and Kountouriotis, P. A., "A stochastic approach to dynamic-demand refrigerator control," *IEEE Trans. Control Syst. Technol.*, Vol. 20, No.3, pp. 581-592, June 2012.

[9] Dhanalakshmi, R., and Palaniswami, S., "Application of multi stage fuzzy logic control for load frequency control of an isolated wind diesel hybrid power system," *Proc. Int. Conf. on GTEC*, pp. 309-315, Chennai, India, 15-17 December 2011.

[10] Ma, K., Hu, G., and Spanos, C. J., "Distribution energy consumption control via real-time pricing feedback in smart grid," *IEEE Trans. Control Syst. Technol*, Vol. 22, No.5, pp. 1907-1914, September 2014.

[11] Short, J. A., Infield, D. G., and Freris L. L., "Stabilization of grid frequency through dynamic demand control," *IEEE Trans. Power Syst.*, Vol. 22, No. 3, pp. 1284-1293, August. 2007.

[12] Pourmousavi, S. A., and Nehrir, M. H., "Introducing dynamic demand response in the LFC model," *IEEE Trans. Power Syst.*, Vol. 29, No. 4, pp. 1562-1572, July. 2014.

[13] Albadi, M. H., and El-Saadany, E. F., "A summary of demand response in electricity markets," *Electron. Power Syst. Res.*, Vol. 78, No. 11, pp. 1989-1996, November 2008.

[14] Black, J. W., and Ilic, M., "Demand-based frequency control for distributed generation," *Proc. IEEE PES Summer Meeting*, pp. 427-432, 21-25 July 2002.

[15] US DoE, "Benefit of demand response in electricity markets and recommendations for achieving them," *Report to the US Congress*, February 2006. Available http://eetd.idi.gov.

[16] Jay, D., and Swarup, K. S., "Frequency restoration using dynamic demand control under smart grid environment," *Proc. IEEE PES ISGT*, pp. 311-315, Kollam, India, 1-3 December 2011.

[17] Wang, D., Parkinson, S., Miao, W., Jia, H., Crawford, C., and Djilali N., "Online voltage security assessment considering comfort-constrained demand response control of distributed heat pump systems," *Applied Energy*, Vol. 96, No. 18-19, pp. 104-114, August 2012.

[18] Kondoh, J., Lu, N., and Hammerstorm, D. J., "An evaluation of the water heater load potential for providing regulation service," *IEEE Trans. Power Syst.*, Vol. 26, No.3, pp. 1309-1316, August. 2011.

[19] Lu, N., "An envalution of the HVAC load potential for providing load balancing service," *IEEE Trans. Smart Grid*, Vol. 3, No. 3, pp. 1263-1270, September 2012.

[20] Lu, N., and Zhang, Y., "Design considerations of a centralized load controller using thermostatically controlled appliances for continuous regulation reserves," *IEEE Trans. Smart Grid*, Vol. 4, No. 2, pp. 1949-3053, June 2013.

[21] Lu, N., Du, P., and Makarov, Y. V., "The potential of thermostatically controlled appliances for intra-hour energy storage applications," *Proc. IEEE PES General Meeting 2012*, pp. 1-6, San Diego, U.S., 22-26 July 2012.

[22] Rijcke, S. D., Vos, K. D., and Drisen, J., "Balancing wind power with demand-side response," Katholieke University Leuven, February 2010.

[23] Molina-Garcia A., Munoz-Benavente, I., Hansen, A. D., and Gomez-Lazaro, E., "Demand-side contribution to primary frequency control with wind farm auxiliary control," *IEEE Trans. Power Syst*, Vol. 29, No. 5, September 2014.

[24] Jiang, L., Yao, W., Wu, Q. H., Wen, J. Y., and Cheng, S. J., "Delay-dependent stability for load frequency control with constant and time-varying delays," *IEEE Trans. Power Syst.*, Vol. 27, No. 2, pp. 932-941, May 2012.

[25] Yang, K. Y., Zhang, L. L., and Zhang, J., "Dynamic analysis and control of three dimensional energy supply and demand system with time delay," *Proc. 2014 33rd Chinese Control Conference*, pp. 7121-7126, Nanjing, China, July 2014.

[26] Zhang, C. K., Jiang, L., Wu, Q. H., He, Y., and Wu, M., "Delay-dependent robust load frequency control for time delay power systems," *IEEE Trans. Power Syst.*, Vol. 28, No. 3, pp. 2192-2201, August 2013.

[27] Zhang, C. K., Jiang, L., Wu, Q. H., He, Y., and Wu, M., "Further Results on delay-dependent stability of multi-area load frequency control," *IEEE Trans. Power Syst.*, Vol. 28, No. 4, pp. 4465-4474, November 2013.

[28] Yao, W., Jiang, L.,Wu, Q. H., Wen, J. Y., and Cheng, S. J., "Delay-dependent stability analysis of the power system with a wide-area damping controller embedded," *IEEE Trans. Power Syst.*, Vol. 26, No. 1, pp. 233-240, January 2011.

[29] Yao, W., Jiang, L., Wen, J. Y., Wu, Q. H., and Cheng, S. J., "Wide-area damping controller of FACTS devices for inter-area oscillations considering communication time delays," *IEEE Trans. Power Syst.*, Vol. 29, No. 1, pp. 318-329, January 2014.

[30] Yao, W., Jiang, L., Wen, J. Y., Wu, Q. H., and Cheng, S. J., "Wide-area damping controller for power system inter-area oscillations: a networked predictive control approach," *IEEE Trans. Control Syst. Technol.*, Vol. 23, No. 1, pp. 27-36, January 2015.

[31] Ramakrishnan, K., and Ray, G., "Improved results on delay-dependent stability of LFC systems with multiple time delays," *J. Control Autom. Electr. Syst.*, Vol. 26, No. 3, pp. 235-240, February 2015.

[32] Shayeghi, H., Shaynfar, H. A., and Jalili, A., "Multi-stage fuzzy PID power system automatic generation controller in deregulated environment," *Energy Convers. Manage.*, Vol. 47, No. 18-19, pp. 2829-2845, November 2006.

[33] Zhu, Q., Yao, W., Jiang, L., Luo C., and Wu, Q. H., "Load frequency control with dynamic demand control for deregulated power system," *Proc. 2014 IEEE PES General Meeting*, Washington DC, U.S., pp. 1-5, 27-31 July 2014.

[34] Samarakoon, K., Ekanayake J., and Jenkins, N., "Investigation of domestic load control to provide primary frequency response using smart meters," *IEEE Trans. Smart Grid*, Vol. 3, No. 1, pp. 282-292, March 2012.

[35] Zhang, W., Kalsi, K., Fuller, J., Elizondo, M., and Chassin, D., "Aggregate model for heterogeneous thermostatically controlled loads with demand response," *Proc. 2012 PES General Meeting*, pp. 1-8, San Diego, U.S., 22-26 July 2012.

[36] Lu, N., Chassin, D. P., and Widergren, S. E., "Modeling uncertainties in aggtrgated thermoststically controlled loads using a state queueing model," *IEEE Trans. Power Syst.*, Vol. 20, No.2, pp. 725-733, May 2005.

[37] Ting, T., Rao, M., and Loo, C. "A novel approach for unit commitment problem via an effective hybrid particle swarm optimization," *IEEE Trans. Power Syst.*, Vol. 21, No.1, pp. 411-418, February 2006.

Biographies

Qi Zhu received the B.Sc. degree in electrical engineering and automation from the University of Liverpool, Liverpool, UK, and Xian Jiaotong-Liverpool University, Suzhou, China, in 2012. She is currently pursuing the Ph.D. degree at the University of Liverpool. Her research interests include demand side management, power system stability analysis and control, and renewable energy.

Lin Jiang received the B.Sc. and M.Sc. degrees from Huazhong University of Science and Technology, Wuhan, China, in 1992 and 1996, respectively, and the Ph.D. degree from the University of Liverpool, Liverpool, UK, in 2001, all in electrical engineering. He is currently a Senior Lecturer with the Department of Electrical Engineering and Electronics, University of Liverpool. His research interests include advanced control and applications in power system, smart grid, and renewable energy.

Wei Yao received the B.Sc. and Ph.D. degrees in electrical engineering from Huazhong University of Science and Technology (HUST),Wuhan, China, in 2004 and 2010, respectively. He was a Post-Doctoral Researcher with the Department of Power Engineering, HUST, from

2010 to 2012, where he is currently an Associate Professor with the School of Electrical and Electronics Engineering. He was a Post-Doctoral Research Associate with the Department of Electrical Engineering and Electronics, University of Liverpool, Liverpool, UK, from 2012 to 2014. His research interests include power system stability analysis and control, renewable energy, and HVDC and FACTS.

Chuan-Ke Zhang received the B.Sc. degree in automation and the Ph.D. degree in control science and engineering from Central South University, Changsha, China, in 2007 and 2013, respectively. He is an Associate Professor with the School of Automation, China University of Geosciences,Wuhan, China. His research interests include time-delay systems, chaos synchronization, and power system stability and control.

Cheng Luo received the B.Sc. and M.Sc. degrees from Huazhong University of Science and Technology (HUST), Wuhan, China, in 2000 and 2002, respectively, both in electrical engineering; and the Ph.D. degree in electrical engineering with a minor in applied mathematics from Iowa State University, Ames, IA, USA, in 2011. Currently, he is with the Department of Forward Operations, Midcontinent Independent System Operator, Inc. (MISO), Cormel, IN, USA. His research interests include electricity market operations, power system stability, optimization, and state estimation.